Zona incerta neurons projecting to the ventral tegmental area promote action initiation towards feeding

Kathy C.G. de Git[1], Esther M. Hazelhoff[1], Minke H.C. Nota[1], Erik Schele[2], Mieneke C.M. Luijendijk[1], Suzanne L. Dickson[2], Geoffrey van der Plasse[1,*] and Roger A.H. Adan[1,2,*]

[1]*Department of Translational Neuroscience, Brain Center Rudolf Magnus, University Medical Center Utrecht, Utrecht University, Utrecht, The Netherlands*
[2]*Institute of Neuroscience and Physiology, Sahlgrenska Academy, University of Gothenburg, Medicinaregatan 11, Göteborg, 41390, Sweden*

Edited by: Katalin Toth & Weifang Rong

The Journal of Physiology

> **Key points**
>
> - The zona incerta (ZI) and ventral tegmental area (VTA) are brain areas that are both implicated in feeding behaviour. The ZI projects to the VTA, although it has not yet been investigated whether this projection regulates feeding.
> - We experimentally (in)activated the ZI to VTA projection by using dual viral vector technology, and studied the effects on feeding microstructure, the willingness to work for food, general activity and body temperature.
> - Activity of the ZI to VTA projection promotes feeding by facilitating action initiation towards food, as reflected in meal frequency and the willingness to work for food reward, without affecting general activity or directly modulating body temperature.
> - We show for the first time that activity of the ZI to VTA projection promotes feeding, which improves the understanding of the neurobiology of feeding behaviour and body weight regulation.

Abstract Both the zona incerta (ZI) and the ventral tegmental area (VTA) have been implicated in feeding behaviour. The ZI provides prominent input to the VTA, although it has not yet been investigated whether this projection regulates feeding. Therefore, we investigated the role of ZI to VTA projection neurons in the regulation of several aspects of feeding behaviour. We determined the effects of (in)activation of ZI to VTA projection neurons on feeding microstructure, food-motivated behaviour under a progressive ratio schedule of reinforcement, locomotor activity and core body temperature. To activate or inactivate ZI neurons projecting to the VTA, we used a combination of canine adenovirus-2 in the VTA, as well as Cre-dependent designer receptors exclusively activated by designer drugs (DREADD) or tetanus toxin (TetTox) light chain in the ZI. TetTox-mediated inactivation of ZI to VTA projection neurons reduced food-motivated behaviour and feeding by reducing meal frequency. Conversely, DREADD-mediated chemogenetic activation of ZI to VTA

Kathy de Git is interested in medical physiology and neuroscience. She obtained her PhD at the Department of Translational Neuroscience, Utrecht University, where she studied hypothalamic control of energy balance. A variety of strategies (pharmacogenetics, viral vector technology, *in vivo* electrophysiology, optogenetics and automated behavioural and physiological analysis) were used to unravel mechanisms underlying feeding behaviour.

*These authors contributed equally to this work.

projection neurons promoted food-motivated behaviour and feeding. (In)activation of ZI to VTA projection neurons did not affect locomotor activity or directly regulate core body temperature. Taken together, ZI neurons projecting to the VTA exert bidirectional control overfeeding behaviour. More specifically, activity of ZI to VTA projection neurons facilitate action initiation towards feeding, as reflected in both food-motivated behaviour and meal initiation, without affecting general activity.

Introduction

The worldwide prevalence of obesity is steadily increasing (Nguyen & El-Serag, 2010). In our modern society, a sedentary lifestyle combined with calorie over-consumption plays an important role in the aetiology of obesity (Naef *et al.* 2015; Romieu *et al.* 2017). Under-standing the neurobiology of different aspects of feeding behaviour, such as motivational drive, satiety and the anticipation to food, is a first step to tackle the obesity epidemic (Kelley *et al.* 2005; van Zessen *et al.* 2012).

Among neural circuits regulating feeding, the mesolimbic dopamine (mesDA) system has been implicated in food motivation (Wise, 2004, Berridge, 2007, Salamone and Correa, 2012, van Zessen *et al.* 2012, Meye and Adan, 2014, Boekhoudt *et al.* 2017). The mesDA system consists of dopaminergic neurons in the ventral tegmental area (VTA) that project to cortico-limbic structures such as the ventral striatum (van Zessen *et al.* 2012, Boekhoudt *et al.* 2017). DA is an important modulator of feeding behaviour. DA-deficient mice starve to death without additional treatment with the dopamine precursor L-DOPA (Zhou & Palmiter, 1995). Conversely, alterations in the mesDA system, such as reduced DA D2 receptor expression in the striatum, have been associated with overconsumption and obesity in both animals and humans (Wang *et al.* 2001, Volkow *et al.* 2008, Johnson and Kenny, 2010, Stice *et al.* 2010, Cone *et al.* 2013, McCutcheon, 2015). The precise role of VTA DA signalling in the control of food intake is incompletely understood, although VTA DA signalling is at least crucially involved in the motivation to work for food (Wise, 2004, Berridge, 2007, Salamone and Correa, 2012, Meye and Adan, 2014, Boekhoudt *et al.* 2018) and was shown to facilitate both the initiation and cessation of feeding (Boekhoudt *et al.* 2017).

The VTA receives input from metabolic centres located in the hypothalamus that regulate feeding behaviour and energy balance (van Zessen *et al.* 2012, Meye and Adan, 2014, van der Plasse *et al.* 2015). The lateral hypothalamus (LH) and zona incerta (ZI) provide the major direct hypothalamic innervation of the VTA (Gonzalez *et al.* 2012,

Ogawa *et al.* 2014). Although the LH>VTA projection has been extensively studied (Ferrario *et al.* 2016), the ZI>VTA projection has not yet been investigated. The first evidence for a role of the ZI in feeding behaviour was provided by ZI lesion studies in rats, which resulted in a reduction in *ad libitum* feeding and body weight (Huang & Mogenson, 1974, McDermott and Grossman, 1979; but see also Mitrofanis, 2005). In addition, studies in sheep showed that the ZI responds to the ingestion and especially the sight of food by releasing GABA (Kendrick *et al.* 1986, Kendrick *et al.* 1991). Recently, stimulation of ZI GABA neurons was shown to evoke binge-like eating and body weight gain in mice (Zhang & van den Pol, 2017). Also, patients with Parkinson's disease receiving deep brain stimulation of the subthalamus, including the ZI, sometimes show binge-like eating (Zahodne *et al.* 2011, Amami *et al.* 2015). Thus, several lines of evidence indicate that the ZI is involved in feeding and energy balance. The ZI has robust projections throughout the brain (Mitrofanis, 2005) and was previously shown to mediate feeding behaviour via projections to the paraventricular thalamus (Zhang & van den Pol, 2017), although the role of its projections to the VTA has not yet been studied.

In the present study, we investigated whether the ZI projections to the VTA regulate feeding behaviour. Several aspects of feeding behaviour, including the motivation to work for food and feeding microstructure, were assessed. Locomotor activity and body temperature were also tested to determine whether ZI>VTA projection neurons specifically mediate feeding behaviour, or also have a role in energy metabolism. We first permanently inactivated ZI>VTA projection neurons using a combination of canine adenovirus 2 (CAV2Cre) in the VTA (Hnasko *et al.* 2006, Boender *et al.* 2014, Boekhoudt *et al.* 2016) and Cre-dependent tetanus toxin (TetTox) light chain in the VTA (Carter *et al.* 2015, Campos *et al.* 2017). Then, we tested whether chemogenetic activation of ZI>VTA projection neurons, by the combined use of CAV2Cre in the VTA and Cre-dependent designer receptors exclusively activated by designer drugs (DREADD) in the ZI (Hnasko *et al.* 2006, Boender *et al.* 2014,

Boekhoudt *et al.* 2016), results in opposite effects on feeding behaviour.

Methods

Animals and ethical approval

Upon arrival, adult male Wistar rats (Charles-River, Sulzfeld, Germany) were group housed in a temperature (21–23°C) and light controlled (lights on between 13.00 h and 01.00 h) room. At the time of surgery, rats weighed 385 ± 5 g in experiment 1 and 484 ± 10 g in experiment 2. Following surgery, rats were housed individually in Plexiglas cages. Rats had *ad libitum* access to pelleted rat chow (3.31 kcal g^{-1}; Special Diet Service, Witham, UK) and tap water, unless stated otherwise. In experiment 1, rats were food restricted from weeks 11 to 16, during which rats received 4 g of chow per 100 g of body weight. All experiments were approved by the Animal Ethics Committee of Utrecht University and conducted in agreement with Dutch laws (Wet op de Dierproeven, 1996; revised 2014) and European regulations (Guideline 86/609/EEC; Directive 2010/63/EU).

Experiment 1: Inactivation of the ZI-region to VTA projection neurons

Surgery: inactivating ZI-region to VTA projection neurons. The first group consisted of 18 rats, which were randomly divided into two subgroups of nine rats based on their average body weight and the motivation to work for food rewards (number of rewards) during operant conditioning in the 2 weeks before surgery. The first sub-group, referred to as the TetTox group, was bilaterally injected with 1.0 μL of AAV-CBA-DIO-GFP:TetTox (hereafter abbreviated as Cre-dependent TetTox-GFP; 1.0×10^{12} genomic copies mL^{-1}), kindly provided by Richard D. Palmiter (Carter *et al.* 2015) in the ZI, and bilaterally injected with 0.3 μL of a mixture of CAV2cre (final concentration in mixture 1.25×10^{12} genomic copies mL^{-1}; IGMM, Montpellier, France) and AAV-hSyn-mCherry (final concentration in mixture 1.0×10^{12} genomic copies mL^{-1}; UNC Vector Core, Chapel Hill, NC, USA) in the VTA. The second subgroup, referred to as the control group, was bilaterally injected with 0.3 μL of AAV-hSyn-DIO-hM3D(Gq)-mCherry (1.0×10^{12} genomic copies mL^{-1}; UNC Vector Core) in the ZI, and bilaterally injected with 0.3 μL of a mixture of CAV2cre (final concentration in mixture 1.25×10^{12} genomic copies mL^{-1}; IGMM) and AAV-hSyn-YFP (final concentration in mixture 1.0×10^{12} genomic copies mL^{-1}; UNC Vector Core) in the VTA. For both subgroups, the same co-ordinates were used for the ZI [from bregma: anterior-posterior (AP): -2.30 to -2.50 mm,

medio-lateral (ML): $+1.40$ mm, dorso-ventral (DV): -9.30 mm, at an angle of 5°] and the VTA (from bregma: AP: -5.40 mm, ML: $+2.20$ mm, DV: -8.90 mm, at an angle of 10°). Because there were no differences observed between virus expression and behavioural measures between the different AP co-ordinates, they were considered to be equal and combined for statistical analyses. In addition, an intra-abdominal transmitter (TA10TA-F40; Data Science International, Saint Paul, MN, USA) was implanted to continuously monitor core body temperature and locomotor activity.

An additional histology experiment was performed to demonstrate that targeting of the ZI to VTA projection was specific and did not spread to other known projection areas, such as paraventricular thalamus. For this experiment, we injected four rats with 0.3 μL of CAV2cre (final concentration in mixture 1.25×10^{12} genomic copies mL^{-1}; IGMM) into the VTA and 1 μL AAV-CBA-DIO-GFP:TetTox in the ZI.

Surgery was performed under fentanyl/fluanisone (0.315 mg kg^{-1} fentanyl, 10 mg kg^{-1} fluanisone; Hypnorm, Janssen Pharmaceutica, Belgium) and midazolam (2.5 mg kg^{-1}, I.P., Actavis, Haarlem, The Netherlands) anaesthesia. Xylocaine was sprayed on the skull to provide local anaesthesia (Lidocaine 100 mg ml^{-1}; AstraZeneca BV, The Hague, The Netherlands). All rats received three daily peri-surgical injections of carprofen (5 mg kg^{-1}, s.c. Carporal; AST Farma BV, Oudewater, The Netherlands), starting at the day of surgery.

Operant conditioning: testing the motivation to work for food rewards.

Apparatus. Experiments were conducted in two-lever operant conditioning chambers designed for rats (30.5 × 24.1 × 21.0 cm; Med Associates, St Albans, VT, USA), which were placed in light- and sound-attenuating cubicles equipped with a ventilation fan. Each chamber was equipped with a metal grid floor, two retractable levers with a cue light above each lever, a pellet dispenser to deliver sucrose pellets (45 mg; TestDiet, St Louis, MO, USA) to a receptacle between the two levers and a house light. Data collection and processing was controlled by MED-PC software (Med Associates).

Training. Starting ~6 weeks before surgery, rats learned to lever press for sucrose pellets under a fixed ratio (FiR)1 schedule, as described previously (la Fleur *et al.* 2007). During each trial, both levers were present, although only presses on the active lever (ALPs) led to delivery of a sucrose pellet, illumination of the cue light above the active lever and retraction of both levers. Twenty seconds after the pellet was received, the levers were reinserted into the chamber. Presses on the inactive lever (ILPs) were recorded but had no consequence. After acquisition of sucrose self-administration under this

schedule, rats were further trained on a FiR3 schedule and then on a FiR5 schedule, where the response requirement to obtain a sucrose pellet was increased to three and five ALPs, respectively. All sessions lasted 30 min or until rats had earned the maximum number of pellets (i.e. 60 for FiR1 and FiR3; 30 for FiR5), whichever occurred first. Four weeks before surgery, all rats were considered trained and a progressive ratio (PR) schedule was implemented.

PR. The effort rats were willing to make for a sucrose reward was tested under a PR schedule, in which the response requirement to obtain a sucrose pellet was progressively increased after each obtained reward (1, 2, 4, 9, 12, 15, 20, 25, 32, 40, 50, 62, 77, 95, 118, 145, 178, 219, 268, 328, 402, 492, 603 and 737) (la Fleur *et al.* 2007). The session ended when the rat had failed to earn a reward within 30 min. All PR sessions started before 12.00 h and were completed before 13.00 h. Rats of the control and TetTox group were equally divided over the chambers and sessions. PR responding was assessed 5 days per week for 4 weeks prior to virus injections. Four weeks after virus injections, PR testing recommenced and was assessed 3 days per week, both under *ad libitum* feeding (week 4–9) and restricted feeding in the home cage (weeks 12–16).

Feeding patterns: measuring feeding microstructure. Feeding behaviour was studied using data collected by Scales (Department Biomedical Engineering, UMC Utrecht, The Netherlands) (van der Zwaal *et al.* 2010, la Fleur *et al.* 2014). This program records the weight of food hoppers in the home cage automatically every 12 s. To study feeding behaviour without interference by behavioural tasks or handling, weekend data were analysed for each week. Feeding microstructure was analysed from weeks 6 to 9 during *ad libitum* feeding. As reported previously (van der Zwaal *et al.* 2010, la Fleur *et al.* 2014), a meal was defined as an episode of food intake with a minimal consumption of 1 kcal (0.3 g of chow) and a minimal inter-meal interval of 5 min.

Telemetric measurements: locomotion and temperature measurement. Each home cage was placed on a receiver plate (DSI, St Paul, MN, USA) that received radio-frequency signals from the abdominal transmitter. The plates were connected to software (DSI) that recorded core body temperature and locomotor activity every 10 min. To study telemetry data without interference by behavioural tasks or handling, 48 h weekend data was analysed for each week, and detailed telemetry data per hour was analysed for weeks 6–9.

Tissue preparation: checking virus injection sites. During week 29 post-surgery, rats were given a lethal dose of sodium pentobarbital (100 mg kg^{-1}, Euthanimal; Alfasan BV, Woerden, The Netherlands) and were trans-cardially perfused with 0.9% NaCl followed by 4% paraformaldehyde in PBS. Brains were excised and kept in 4% paraformaldehyde for 24 h, and were subsequently saturated with 30% sucrose in PBS with 0.01% NaN3. Brains were snap frozen in isopentane between −60°C and −40°C and sliced into 40 μm sections using a cryostat (Leica Microsystems, Wetzlar, Germany). Tissue was collected in six series in cryo-protectant (25% glycerol; 25% ethylene-glycol in PBS) and stored at −20°C.

Immunohistochemistry: checking virus injection sites. One series of brain slices was washed in PBS and subsequently blocked and permeabilized in blocking solution (PBS containing 10% fetal calf serum and 1% Triton X-100) for 2 h. Subsequently, slices were incubated overnight at 4°C with primary chicken anti-GFP antibody (dilution 1:500; Abcam, Cambridge, UK) and rabbit anti-dsRed (dilution 1:500; Clontech, Palo Alto, CA, USA) in blocking solution. After washing in PBS, brain slices were incubated with Alexa-488 labelled secondary goat anti-chicken and Alexa-568 labelled goat anti-rabbit (dilution 1:500; Abcam) antibodies in blocking solution for 2 h. After washing in PBS, slices were mounted on SuperFrost glasses (VWR, Leuven, Belgium) and covered with FluorSave (Millipore, Burlington, MA, USA).

***In situ* hybridization: checking virus injection sites.** *In situ* hybridization (ISH) was performed for the detection of (floxed) GFP expressed by the AAV-CBA-DIO-GFP:TetTox virus in the ZI-region. One series of (perfused) brain slices was washed in PBS, acetylated for 10 min and washed again in PBS. Slices were pre-hybridized in hybridization solution [50% formamide, 5 × saline-sodium citrate (SSC), 5 × Denhardt's, 250 μg mL^{-1} tRNA Baker's yeast, 500 μg mL^{-1} sonificated salmon sperm DNA] for 2 h at room temperature. Subsequently, slices were incubated overnight at 68°C in hybridization solution containing 400 ng mL^{-1} 720 bp long digoxigenin-labelled enhanced green fluorescent protein probe riboprobe (antisense to NCBI gene DQ768212). Slices were quickly washed in pre-warmed (68°C) 2 × SSC and then incubated in pre-warmed 0.2 × SSC for 2 h at 68°C. Digoxigenin was detected with an alkaline phosphatase labelled antibody (dilution 1:5000; Roche, Mannheim, Germany) after overnight incubation at room temperature using NBT/BCIP as a substrate. Slices were mounted on SuperFrost glasses (VWR), dehydrated in ethanol, cleared in xylene and embedded in Entellan (Merk Millipore, Burlington, MA, USA).

Histological analysis: checking virus injection sites. Immunofluorescence and ISH slices were photographed and digitized using the epifluorescence and brightfield

function of an Axioskop 2 microscope (Carl Zeiss, Oberkochen, Germany), respectively. The injection site of CBA-DIO-GFP:TetTox in the ZI-region was determined by the expression of GFP RNA positive cell bodies, and the injection site of CAV2cre in the VTA was determined by the expression of cell bodies with mCherry immunoreactivity, resulting from the co-injected AAV-hSyn-mCherry virus.

Experiment 2: Chemogenetic activation of ZI to VTA projections

Surgery: activating ZI to VTA projection neurons. A second group of rats ($n = 14$) underwent surgery using procedures identical to those employed in experiment 1, but they were bilaterally injected with 0.3 μL of the activating DREADD AAV-hSyn-DIO-hM3D(Gq)-mCherry (1.0×10^{12} genomic copies mL^{-1}; UNC Vector Core) in the ZI (from bregma: AP: -2.30 mm, ML: $+1.40$ mm, DV: -8.80 mm, at an angle of 0°) and bilaterally injected with 0.3 μL of a mixture of CAV2cre (final concentration in mixture 1.33×10^{12} genomic copies mL^{-1}; IGMM) and AAV-hSyn-YFP (final concentration in mixture 1.60×10^{12} genomic copies mL^{-1}; UNC Vector Core) in the VTA (from bregma: AP: -5.40 mm, ML: $+2.20$ mm, DV: -8.90 mm, at an angle of 10°).

Drugs. Clozapine-*N*-oxide (CNO; kindly provided by Bryan Roth and NIMH) was dissolved to a concentration of 0.3 mg mL^{-1} in sterile saline (0.9% NaCl). All injections were given I.P., and the effect of CNO and saline injections on PR responding, feeding behaviour, locomotor activity and body temperature was tested according to a Latin square design. Rats received two habituation saline injections (I.P.) prior to testing.

Operant conditioning: testing the motivation to work for food rewards. PR training was performed via procedures identical to those employed in experiment 1. PR testing recommenced 2.5 weeks after virus injections, and the effect of CNO *vs.* saline on PR responding was assessed 4 weeks after virus injections. Rats were injected 30 min before being placed in the operant chambers. At least one washout day was kept between injections.

Feeding patterns and telemetric measurements: feeding microstructure, locomotion and temperature measurement. The effect of CNO on feeding behaviour was tested during the same test session as that for body temperature and locomotor activity. Telemetry data were recorded every 2 min. During a test session, body temperature and activity were first measured in the absence of food to prevent confounding with feeding-induced thermogenesis. Rats were food restricted at 9.00 h, injected with saline or CNO at 14.30 h and food was returned at 15.30 h. Rats were once habituated to the test schedule prior to testing. Testing commenced 7 weeks after virus injections and the interval between the two test sessions of a Latin square design was at least 4 days. Feeding patterns were analysed up to 6 h following food return.

Tissue preparation: checking virus injection sites. During week 10 post-surgery, rats were transcardially perfused and tissue was prepared via procedures identical to those employed in experiment 1.

Immunohistochemistry: checking virus injection sites. One series of brain slices was washed in PBS, blocked and permeabilized in blocking solution (PBS containing 10% normal goat serum and 1% Triton X-100) for 1 h, and washed again in PBS. Subsequently, slices were incubated overnight at 4°C with primary chicken anti-GFP antibody (dilution 1:500; Abcam) and rabbit anti-dsRed (dilution 1:500; Clontech) in carrier solution (PBS containing 3% normal goat serum and 0.25% Triton X-100). After washing in PBS, brain slices were incubated with Alexa-488 labelled secondary goat anti-chicken and Alexa-568 labelled goat anti-rabbit (dilution 1:500; Abcam) antibodies in carrier solution for 1 h. After washing in PBS, slices were mounted on SuperFrost glasses (VWR) and covered with FluorSave (Millipore).

Histological analysis: checking virus injection sites. Histological analysis was performed as described in experiment 1. The injection site of AAV-hSyn-DIO-hM3D(Gq)-mCherry was determined by the expression of mCherry positive cell bodies, and the injection site of CAV2cre in the VTA was determined by the expression of cell bodies with GFP immunoreactivity, resulting from the co-injected AAV-hSyn-YFP virus.

Statistical analysis. In experiment 1, differences in PR performance, feeding behaviour, body weight and telemetric measurements were tested by performing two-way repeated measures ANOVAs (RM ANOVAs) with time as within-subject variable and group (control; TetTox) as between-subject variable. In experiment 2, differences in these parameters were tested by performing a paired *t* test with treatment as within-subject variable or a two-way repeated measures ANOVAs with treatment and time as within-subject variables.

Mauchly's test of sphericity was used to test whether variances of the differences between treatment levels were equal. If the assumption of sphericity was violated, degrees of freedom were corrected using Greenhouse–Geisser estimates of sphericity or Huynh–Feldt estimates of

sphericity when the Greenhouse–Geisser estimate was >0.75. When appropriate, *post hoc* analyses were conducted using Student's *t* tests or pairwise Bonferroni comparisons. Each parameter was tested for normality with the Kolmogorov–Smirnov test. When data were not normally distributed, data were transformed using a square root for count data and log transformation for the other data prior to statistical analyses.

Statistical analyses were conducted using SPSS, version 20.3 (IBM Corp., Armonk, NY, USA). $P < 0.05$ was considered statistically significant. Data are presented as the mean ± SD.

In experiment 1, one rat of the control group died shortly after surgery. We selected rats with bilateral expression in the ZI. In many rats infection spread to surrounding areas, often to the dorsomedial hypothalamus (DMH). Three rats of the TetTox group did not show GFP expression in the ZI because staining was in the DMH, and therefore they were excluded from all analyses. Because of technical issues with the weighing system, the following food intake data were excluded: baseline for one TetTox rat; week 4 for one control rat; and week 6 for two control and two TetTox rats. To allow testing by repeated measures ANOVAs, the average of week 3/5 and week 5/7 was taken for the affected rats in weeks 4 and 6, respectively. In experiment 2, experiments were performed in two subgroups of rats. The first group consisted of nine rats. The second group of five rats was added later and tested under similar experimental procedures. One rat from this group died shortly after surgery. Because there were no differences observed between virus expression and behavioural measures between the two subgroups, they were considered to be equal and combined for the statistical analyses.

Results

Experiment 1: Inactivation of the ZI-region to VTA projection neurons

Selective inactivation of ZI-region neurons projecting to the VTA. To investigate the role of ZI neurons projecting to the VTA, we aimed to specifically inactivate these neurons by injecting CAV2Cre in the VTA and Cre-dependent TetTox light chain (AAV-DIO-GFP:TetTox) in the ZI (Fig. 1*A*). CAV2cre infects neurons at terminals at the injection site and retrogradely delivers Cre in neurons that project to the area of injection, which subsequently enables the expression of Cre-dependent TetTox in projection neurons (Hnasko *et al.* 2006, Boender *et al.* 2014, Boekhoudt *et al.* 2016). Expression of TetTox prevents neurotransmitter release from infected neurons (Carter *et al.* 2015, Campos *et al.* 2017). Thus, the combined use of Cre-dependent TetTox and CAV2Cre allows for selective and permanent inactivation of ZI neurons projecting to the VTA. Control rats received a non-inactivating virus (AAV-hSyn-DIO-hM3D(Gq)-mCherry) in the ZI and CAV2Cre in the VTA.

Immunohistological staining of mCherry (from AAV-hSyn-mCherry which was co-injected with CAV2Cre) confirmed correct targeting of the VTA in all rats (Fig. 1*B*), but showed no TetTox-GFP positive neurons around the injection site in the ZI. Perhaps we did not observe TetTox-GFP at the protein level because rats were killed a long time after the virus injections. Therefore, we performed ISH to detect TetTox-GFP mRNA expression. TetTox-GFP mRNA expression was present in the ZI, but showed spread in the zone medioventral to the ZI (Fig. 1*C*). As we often observed spread of virus infection to this region which includes the DMH, we use the term ZI-region (Fig 1*C*) to refer to data of rats with proper targeting of the ZI, although where there was variable viral spread through surrounding brain regions. Three rats showed no TetTox-GFP positive neurons in the ZI and were therefore excluded from all analyses. In the remaining six rats, the ZI was targeted.

In an extra experiment, where rats where killed a few weeks after virus injections, we observed TetTox-GFP positive neurons around the injection site in the ZI (Fig. 1*D*). We also performed immunohistochemical staining of GFP to detect fibres in the VTA and other areas that are known projection sites of the ZI, including the paraventricular thalamus (Zhang & van den Pol, 2017). GFP-stained fibres were clearly visible in the VTA (Fig. 1*E*) but were not observed in other known projection areas (Fig. 1*F*).

Inactivation of the ZI-region to VTA projection neurons reduces food-motivated behaviour. To test whether inactivation of ZI-region neurons projecting to the VTA affects food-motivated behaviour, responding for sucrose under a PR schedule of reinforcement was tested. Prior to virus injections, control and TetTox rats did not significantly differ in rewards and ALPs ($t \geq 1.804$, $P \geq 0.096$) (Fig. 2*A* and *B*), although TetTox rats showed a trend for a reduction in ILPs ($t = 2.047$, $P = 0.063$) (Fig. 2*C*). Although these differences did not reach significance, we cannot exclude that the differences in pre-surgical ALPs between groups contributed to the overall difference in motivation to work for sucrose. PR testing recommenced 4 weeks after virus injections to allow for sufficient virus expression and was performed both under *ad libitum* feeding and during food restriction (FR) in the home cage. Immediately following PR retesting, TetTox rats showed a lower number of ALPs and, consequently, they earned fewer rewards than control rats (Fig. 2*A*

and *B*). Reduced PR performance in TetTox rats was maintained over the course of *ad libitum* feeding, as well as during FR. In accordance with studies showing that FR improves PR performance (Wise, 2004, Solinas and Goldberg, 2005, van Zessen *et al.* 2012), control rats obtained more rewards during FR compared to *ad libitum* feeding (week 9: 9.94 ± 1.40 *vs.* week 16: 12.04 ± 1.81; $t = 3.979$, $P = 0.005$). An FR-induced increase in the number of rewards was also observed in TetTox rats (week 9: 5.08 ± 0.58 *vs.* week 16: 6.94 ± 1.47; $t = 2.625$, $P = 0.047$). These findings indicate that TetTox-inactivation of the ZI-region to VTA projection neurons reduces the motivation to work for food rewards.

The overall lower PR performance in TetTox rats was associated with a lower number of ILPs during the first 3 weeks following virus injections, although this trend was already observed prior to virus injections, and the difference with the control group disappeared over time as a result of a gradual reduction in the number of ILPs in the control group (Fig. 2*C*). Taken together, these findings suggest that the lower number of ALPs in TetTox rats did not result from a reduction in general activity but, instead, was the result of a specific reduction in food-motivated behaviour. Accordingly, TetTox rats did not differ from control rats in locomotor activity in the home cage (Fig. 2*D* and *E*). Thus, TetTox-inactivation of the ZI-region to VTA projection neurons reduces food-motivated behaviour independent of general activity.

Inactivation of the ZI-region to VTA projection neurons reduces *ad libitum* feeding. Chow intake in the home cage did not differ between control and TetTox rats before virus injections (Fig. 3*A*). Starting from week 3 post virus injections onwards, TetTox rats ate less chow compared to control rats under *ad libitum* feeding (Fig. 3*A* and *B*). Both the control and TetTox group showed a rhythmic feeding pattern, with higher chow intake in the dark phase compared to the light phase (Fig. 3*B*) and no differences in light/dark phase feeding distribution were observed between the groups (Fig. 3*C*). Because ∼70% of chow was consumed in the dark phase, the lower chow intake in TetTox rats compared to controls was most pronounced in this phase (difference between groups was 3.97 and

Figure 1. TetTox-GFP is expressed in ZI-region neurons projecting to the VTA

A, to selectively inactive ZI neurons projecting to the VTA, CAV2Cre was injected into the VTA and Cre-dependent TetTox-GFP was injected into the ZI. An AAV-hSyn-mCherry virus was injected together with CAV2Cre to visualize the injection site in the VTA. *B*, immunofluorescence of mCherry (red) in the VTA following virus injection of CAV2Cre/AAV-hSyn-mCherry (bregma −5.30 mm). *C*, TetTox-GFP mRNA expression in the ZI and the zone medioventral to the ZI, together representing the ZI-region (bregma −2.12 mm). Because we often observed spread of virus infection to this region which includes the DMH, we use the term ZI-region to refer to data of rats with proper targeting of the ZI, but in which there was variable viral spread through surrounding brain regions. *D*, ZI neurons projecting to the VTA stained for GFP. *E*, ZI projection terminals in the VTA stained for GFP. *F*, absence of ZI projection terminal staining in the paraventricular thalamus (PVT), following staining for GFP. [Colour figure can be viewed at wileyonlinelibrary.com]
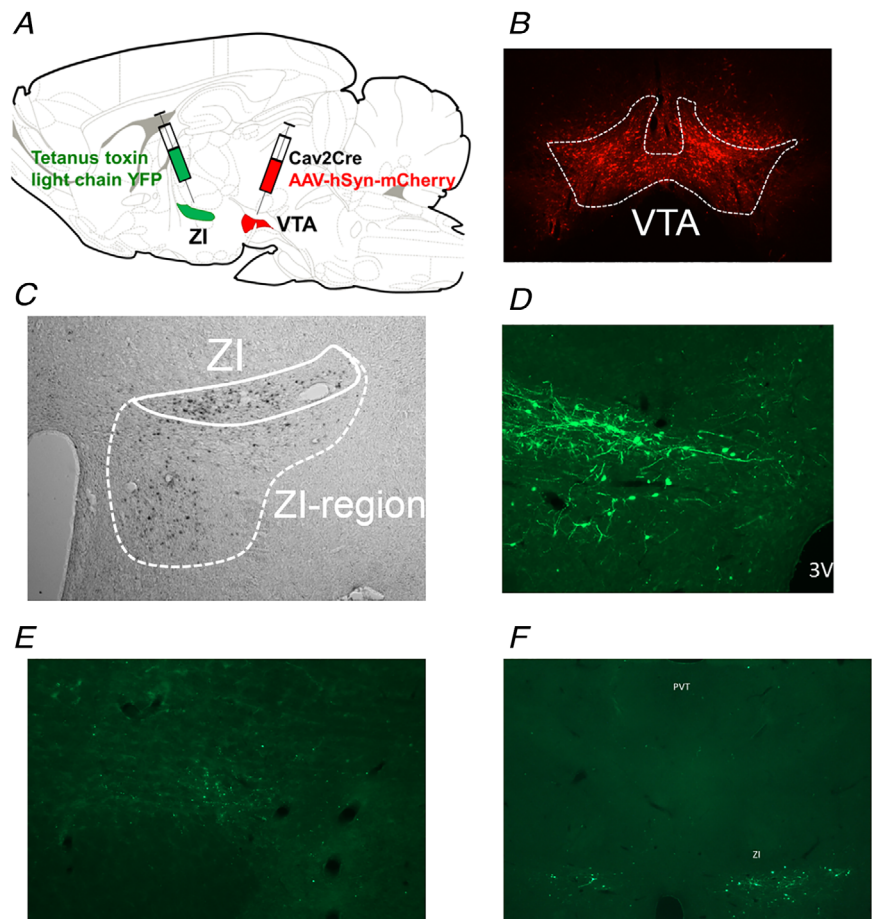
0.97 g in the dark and light phase, respectively) (Fig. 3*B*). A lower chow intake in TetTox rats resulted from a significantly lower number of meals, especially in the dark phase (Fig. 3*D*). TetTox rats showed a non-significant tendency to compensate for their reduced meal frequency by increasing their meal size (Fig. 3*E*), although this was not sufficient to restore food intake levels to those of control rats.

Although all rats increased body weight over the duration of *ad libitum* feeding, body weight was significantly lower in TetTox rats compared to control rats from 7 weeks post virus injections onwards (Fig. 3*F*). Further inspection of the relationship between chow intake and body weight revealed that TetTox rats ate less chow per 100 g of body weight (Fig. 3*G*), suggesting that TetTox rats were metabolically more efficient.

Inactivation of the ZI-region to VTA projection neurons leads to a reduction in core body temperature. From week 3 post virus injections onwards, TetTox rats showed a reduction of $0.32 \pm 0.16°C$ in core body temperature during *ad libitum* feeding compared to

controls (Fig. 4*A*). The timing of the reduction in core body temperature in TetTox rats was similar to that of the reduction in food intake (Figs 3*A* and 4*A*). Core body temperature was significantly reduced during the dark phase (Fig. 4*B*), comprising the period during which the strongest reduction in food intake was observed (Fig. 3*B*). Furthermore, core body temperature correlated significantly with the amount of chow intake during *ad libitum* feeding, especially during the dark phase (Fig. 4*C* and *D*). Taken together, the data show a strong relationship between food intake and core body temperature, which is most apparent during the active feeding period (dark phase).

To further test the correlation between food intake and core body temperature, we challenged rats with FR. Similar to control rats, TetTox rats reduced their core body temperature in response to the reduction in chow intake and the adaptive temperature response did not differ from control rats (Fig. 4*E*).

In summary, TetTox-inactivation of ZI-region neurons projecting to the VTA reduced the motivation to work for food and reduced chow intake as a result of a lower meal
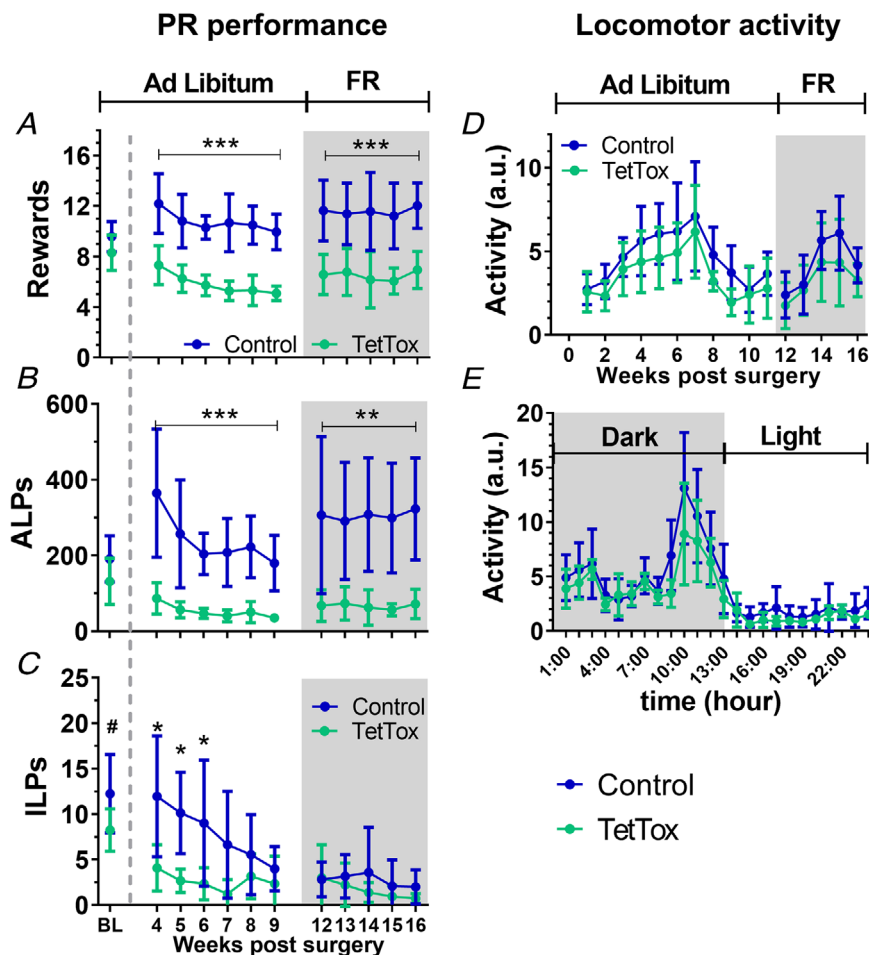
Figure 2. Effect of inactivation of ZI-region neurons projecting to the VTA on responding for sucrose under a PR schedule of reinforcement and locomotor activity
Rewards (*A*), active lever presses (ALPs) (*B*) and inactive lever presses (ILPs) (*C*) in PR testing, averaged per week. Baseline (BL): PR performance 1 week before virus injections (average of five sessions is shown). PR testing recommenced 4 weeks after virus injections, and was assessed under *ad libitum* feeding and food restriction (FR) in the home cage (average of three sessions per week is shown). Statistical analyses were performed by two-way RM ANOVAs, followed by *post hoc* analyses. *Ad libitum*: rewards and ALPs, $F_{group} \geq 51.274$, $P < 0.001$, *post hoc* $P < 0.01$ for all weeks; ILPs, $F_{group} = 10.175$, $P = 0.008$, *post hoc* $P < 0.05$ at weeks 4–6. FR: rewards and ALPs, $F_{group} \geq 21.836$, $P \leq 0.001$, *post hoc* $P < 0.02$ for all weeks; ILPs, $F_{group} = 0.866$, $P = 0.370$. *D*, locomotor activity in arbitrary units (a.u.) averaged per week. *Ad libitum* and FR: $F_{group} \geq 2.683$, $P \geq 0.127$. *E*, locomotor activity over 24 h averaged over the weekend data of weeks 6–9. $F_{group} = 2.337$, $P = 0.152$. Data are shown as the mean ± SD. $n = 8$ for controls and $n = 6$ for TetTox rats. #$P < 0.07$, *$P < 0.05$, **$P < 0.01$, ***$P < 0.06$ compared to controls. [Colour figure can be viewed at wileyonlinelibrary.com]

frequency, without affecting general activity. Food intake showed a strong correlation with core body temperature.

Experiment 2: Chemogenetic activation of ZI>VTA projection neurons

Selective targeting of ZI>VTA projection neurons. We next tested whether chemogenetic activation of the ZI>VTA projection has opposite effects on food-motivated behaviour and *ad libitum* feeding compared to TetTox-inactivation of this projection. Accordingly, Cre-dependent DREADD hM3D(Gq) was injected into the ZI (Fig. 5*A*). CAV2cre was injected into the VTA, where it infects nerve terminals and retrogradely delivers Cre in the ZI, which subsequently enables the expression of Cre-dependent DREADD hM3D(Gq) in ZI neurons projecting to the VTA. Analysis of DREADD hM3D(Gq)-mCherry positive neurons revealed that the ZI was successfully targeted in all rats, and that virus expression was restricted to the ZI (Fig. 5*B*). All of the

rats also showed correct targeting of the VTA (Fig. 5*C*). The core of DREADD hM3D(Gq)-mCherry positive neuron expression in the ZI was observed at −2.3 mm from bregma (range −2.12 to −3.3 mm from bregma) (Table 1).

Chemogenetic activation of ZI>VTA projection neurons promotes food-motivated behaviour. To test whether chemogenetic activation of ZI>VTA projection neurons promotes food-motivated behaviour, responding for sucrose under a PR schedule of reinforcement was tested following treatment with CNO compared to saline, as soon as rats had achieved stable post-surgery PR responding. Rats in experiment 2 were on average less motivated than rats in experiment 1 to lever press to obtain sucrose. We have observed this kind of batch effects before. CNO treatment resulted in a significant increase in the number of ALPs (Fig. 6*B*), leading to a significant increase in the number of rewards earned (Fig. 6*A*). The number of ILPs was not affected by CNO treatment

Figure 3. Effect of inactivation of ZI-region neurons projecting to the VTA on homeostatic feeding

A, chow intake per day, averaged per week, under *ad libitum* feeding and during food restriction (FR). Baseline (BL): paired *t* test $t_{group} = 0.775$, $P = 0.454$; *ad libitum*: RM ANOVA $F_{group} = 22.444$, $P < 0.001$, *post hoc* $P < 0.05$ at weeks 3–9. FR: RM ANOVA $F_{group} = 3.697$, $P = 0.079$. *B*, average chow intake per day during the light and dark phase over the course of *ad libitum* feeding. RM ANOVA $F_{circadian-phase \times group} = 29.066$, $P < 0.001$. *Post hoc*: $P < 0.001$ for total and dark, $P = 0.004$ for light. *C*, percentage (%) of chow intake during the dark and light phase over the course of *ad libitum* feeding. RM ANOVA $F_{circadian-phase \times group} = 0.210$, $P = 0.655$. $F_{circadian-phase} = 139.55$, $P < 0.001$. Number of meals (*D*) and (*E*) meal size averaged over the 24 h weekend data of weeks 6–9. Number of meals: RM ANOVA $F_{circadian-phase \times group} = 10.886$, $P = 0.003$. *Post hoc* $P < 0.01$ for total and dark, $P = 0.090$ for light. Meal size: RM ANOVA $F_{circadian-phase \times group} = 2.707$, $P = 0.111$. $F_{group} = 4.161$, $P = 0.064$. *F*, body weight averaged per week. BL: paired *t* test $t_{group} = 0.004$, $P = 0.997$; *ad libitum*: RM ANOVA $F_{time \times group} = 6.813$, $P = 0.015$, *post hoc* $P < 0.05$ at weeks 7–11. FR: RM ANOVA $F_{time \times group} = 1.002$, $P = 0.353$; $F_{group} = 3.708$, $P = 0.078$. *G*, chow intake per 100 g of body weight per day, averaged per week. BL: paired *t* test $t_{group} = 0.917$, $P = 0.379$; *ad libitum*: RM ANOVA $F_{group} = 26.280$, $P < 0.001$, *post hoc* $P < 0.05$ at weeks 3–7. FR: RM ANOVA $F_{group} = 0.317$, $P = 0.585$. Data are shown as the mean ± SD. $n = 8$ for controls and $n = 5$-6 for TetTox rats. *$P < 0.05$, **$P < 0.01$, ***$P < 0.001$ compared to controls. [Colour figure can be viewed at wileyonlinelibrary.com]
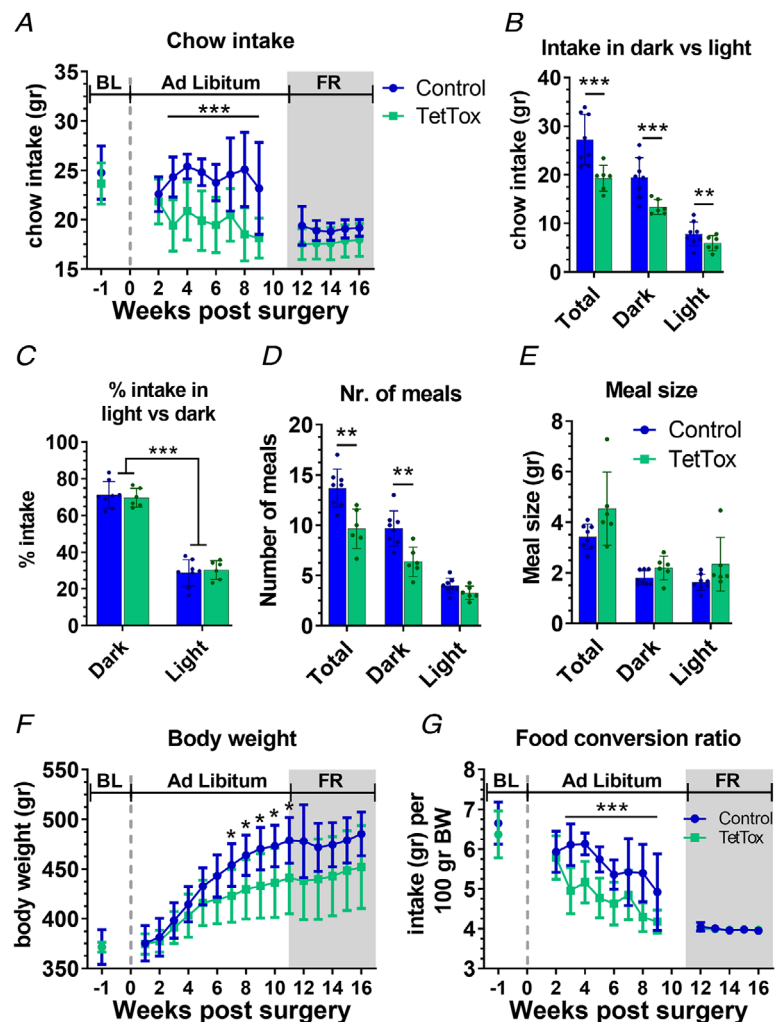
(Fig. 6C), indicating that the CNO-induced increase in ALPs did not result from an increase in general activity. Thus, chemogenetic activation of ZI>VTA projection neurons does not affect general activity (as reflected by ILPs), but specifically increases food reward seeking.

Chemogenetic activation of ZI neurons projecting to the VTA promotes feeding. To test whether chemogenetic activation of ZI neurons projecting to the VTA promotes feeding, rats were injected with saline or CNO following 5.5 h of food restriction. Food was returned 1 h after
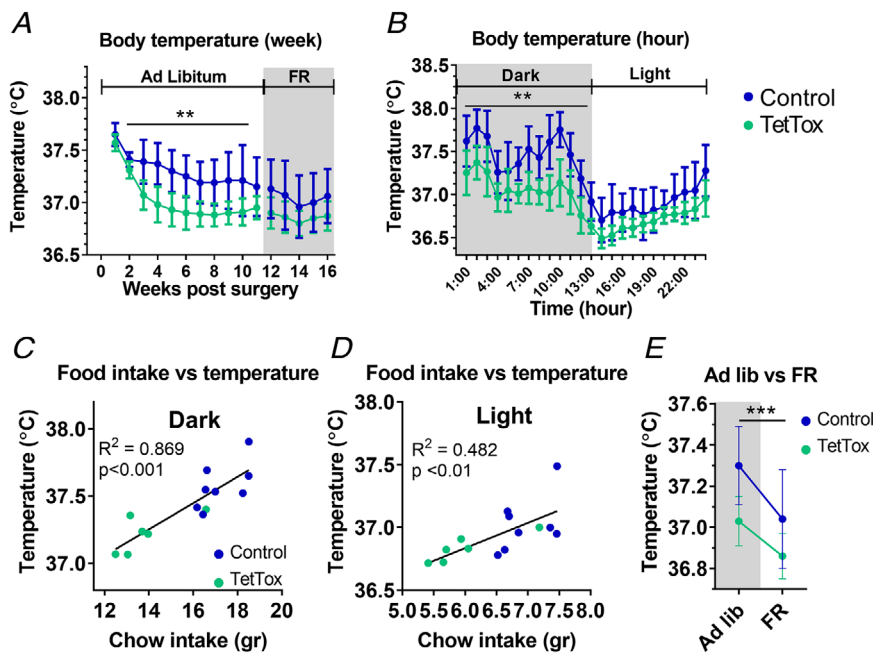
Figure 4. Effect of inactivation of ZI-region neurons projecting to the VTA on body temperature
A, core body temperature during *ad libitum* feeding and food restriction (FR), averaged per week. RM ANOVA $F_{\text{time} \times \text{group}} = 3.754$, $P = 0.026$. *Post hoc* $P < 0.01$ in weeks 3–8, and $P < 0.05$ in weeks 2 and 9. *B*, core body temperature over 24 h averaged over the weekend data of weeks 6–9. RM ANOVA total: $F_{\text{time} \times \text{group}} = 3.154$, $P < 0.001$; dark: $F_{\text{group}} = 17.962$, $P = 0.001$; light: $F_{\text{group}} = 3.581$, $P = 0.083$. *C* and *D*, correlation between food intake and chow intake during the dark and light phase, respectively. *E*, average core body temperature during *ad libitum* feeding and FR. RM ANOVA $F_{\text{feeding-condition} \times \text{group}} = 2.440$, $P = 0.144$. RM ANOVA $F_{\text{feeding-condition}} = 51.808$, $P < 0.001$. Weekend data of weeks 6–9 were analysed. $n = 8$ for controls and $n = 5$-6 for TetTox rats. Data are shown as the mean ± SD. *A* and *B*, **$P < 0.01$ compared to controls. *E*, ***$P < 0.001$ for *ad libitum vs*. FR. [Colour figure can be viewed at wileyonlinelibrary.com]
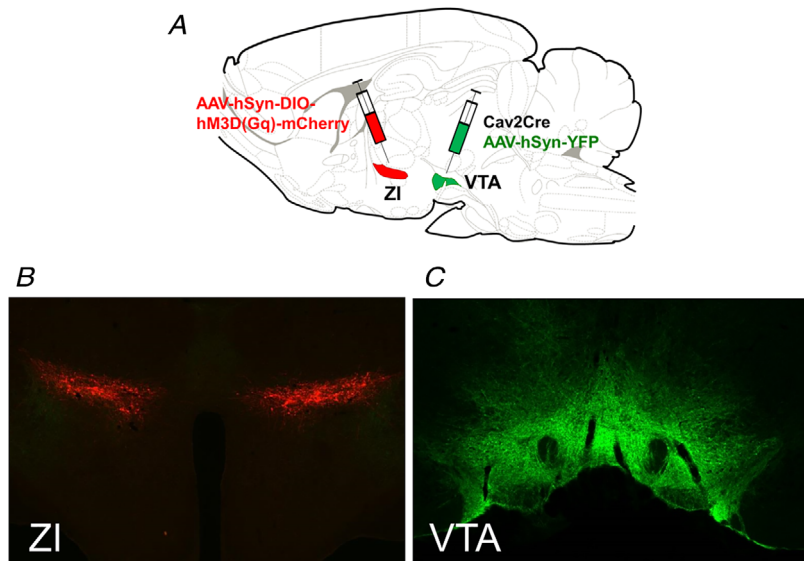
Figure 5. DREADD hM3D(Gq)-mCherry is selectively expressed in ZI neurons projecting to the VTA
A, to selectively inactive ZI neurons projecting to the VTA, CAV2Cre was injected into the VTA and Cre-dependent DREADD hM3D(Gq)-mCherry was injected into the ZI. An AAV-hSyn-YFP virus was injected together with CAV2Cre to visualize the injection site in the VTA. *B*, immunofluorescence of DREADD hM3D(Gq)-mCherry (red) positive neurons in the ZI. *C*, immunofluorescence of GFP (green) in the VTA following virus injection of CAV2Cre/AAV-hSyn-YFP (bregma −5.30 mm). [Colour figure can be viewed at wileyonlinelibrary.com]

Table 1. Expression of mCherry-labelled cell bodies in the ZI

		mm from bregma									
		−1.6	−1.88	−2.12	−2.3	−2.56	−2.8	−3.14	−3.3	−3.6	−3.8
Rat 4	Left	·	x	x	x	x	x	x	x	·	
	Right		x	x	x	·					
Rat 7	Left			·	x	x	·	·	·	·	
	Right		x	x	x	·	·	·	·		
Rat 8	Left		·	x	x	x	x	x	·		·
	Right		·	x	x	x	x	·	·		
Rat 9	Left		x	x	x	x	x	·			
	Right		·	·	x	x	x	·			
Rat 11	Left			x	x	x	x	x	x	·	
	Right		·	·	x	x	x	x	x	·	
Rat 12	Left		x	x	x	x	·	·			
	Right		·	x	x	x	·	·	·		
Rat 15	Left			x	x	x	x	x	x	·	
	Right		·	·	x	x	x	x	x	·	
Rat 17	Left			·	x	x	x	x	x		
	Right		·	x	x	x	x	x	·		
Rat 18	Left		x	x	x	x	·	·			
	Right		x	x	·	·					
Rat 4	Left	·	·	x	x	x	x	x	x	·	
	Right		·	x	x	x	x	x	x	·	·
Rat 6	Left	·	x	x	x	x	x	x	x		
	Right	·	x	x	x	x	x	x	x		
Rat 14	Left		·	x	x	x	x	x	x	x	·
	Right		·	x	x	x	x	x	x	·	
Rat 18	Left		·	x	x	x	x	x	x	x	·
	Right		·	·	x	x	x	x	x	x	·
SUM		0	9	20	25	23	19	16	14	3	0

x, indicates clear cell body expression in the ZI. ·, indicates a few cell bodies in the ZI.

injection, and meal structures were analysed up to 6 h following food return.

All rats typically started feeding immediately (within 2 min) upon access to chow and consumed one meal during the first hour following food return (Fig. 7*A*). The second meal was initiated 2.6 ± 2.09 h after the first meal (Fig. 7*B*). CNO treatment postponed the initiation of the second meal to 4.8 ± 1.49 h after the first meal (Fig. 7*A* and *B*) and significantly increased the first meal size (+1.65 ± 2.46 g difference with saline) (Fig. 7*C*). The satiety ratio (first meal interval/first meal size) shows that post-meal satiety was not affected by CNO treatment (Fig. 7*D*), indicating that, as a result of the larger first meal size with CNO, rats initiated their second meal after a longer first meal interval. The size of the second meal and other meals was not affected by CNO treatment (Fig. 7*C*). In accordance, CNO treatment resulted in a significant increase in cumulative food intake during the first hour after food return only (Fig. 7*E*). As might be expected from such a shor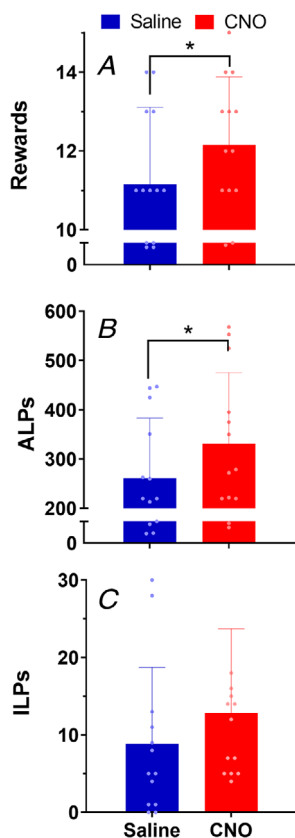t-lasting feeding effect, CNO treatment did not affect 24 h body weight change following injections (data not shown). In summary, chemogenetic activation of ZI>VTA projection neurons promotes feeding by increasing the first meal size specifically.

Chemogenetic activation of ZI>VTA projection neurons does not affect locomotor activity and body temperature. Finally, we tested whether locomotor activity and core body temperature are affected by chemogenetic activation of ZI>VTA neurons. Accordingly, the effects of CNO treatment were assessed in the same test paradigm as for feeding, both before and after food return. No effects of CNO treatment were observed on locomotor activity (Fig. 8*A*) and core body temperature (Fig. 8*B*) in either the absence or presence of food. Thus, these data indicate that chemogenetic activation of ZI>VTA projection neurons primarily stimulates food-related activity, but not general activity, and does not modulate core body temperature.

Discussion

In the present study, we investigated the effects of permanent inactivation and reversible activation of ZI>VTA projection neurons on several aspects of feeding behaviour. TetTox-inactivation of ZI-region neurons projecting to the VTA reduced the motivation to work for food and reduced chow intake as a result of a lower meal frequency, resulting in decreased body weight gain without affecting general activity. These findings suggest that inactivation of ZI>VTA projection neurons specifically reduces food-related action initiation. Chemogenetic activation of ZI>VTA projection neurons resulted in the opposite: increased food-motivated behaviour and feeding, without affecting general activity. Taken together, these findings indicate that ZI>VTA projection neurons drive feeding by facilitating action initiation towards food.

Regulation of feeding behaviour by ZI>VTA projection neurons

Previously, lesioning of the entire ZI-region or of GABA neurons within the ZI resulted in a consistent reduction of *ad libitum food* intake and body weight compared to control rats (Huang & Mogenson, 1974, McDermott and Grossman, 1979, Zhang and van den Pol, 2017; but see also Mitrofanis, 2005). Here, we extend these observations by showing that specific inactivation of the ZI-region to VTA projection neurons results in similar effects, suggesting that the ZI regulates feeding behaviour and body weight via its projections to the VTA.

The reduction in food intake following inactivation of the ZI-region to VTA projection neurons was caused by a reduction in meal frequency, indicating reduced
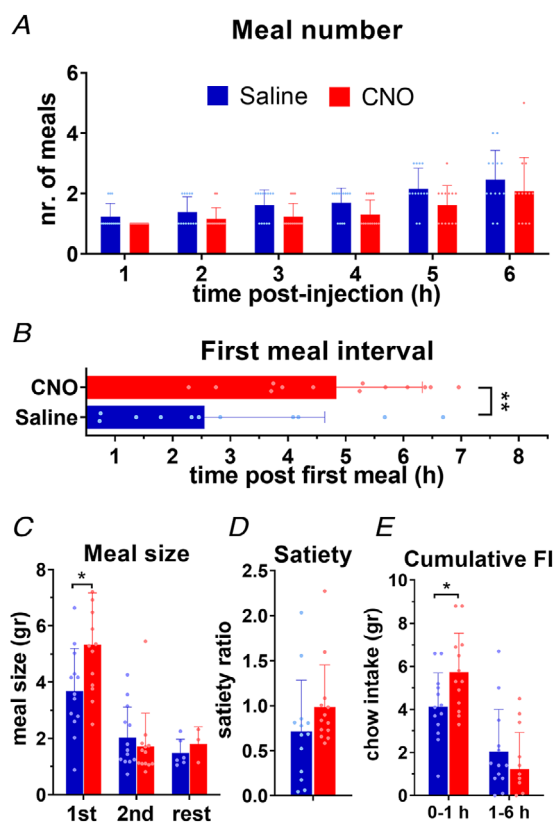

Figure 6. Effect of chemogenetic activation of ZI to VTA projection neurons on responding for sucrose under a PR schedule of reinforcement
Rewards (*A*), active lever presses (ALPs) (*B*) and inactive lever presses (ILPs) (*C*) in PR testing following saline and CNO injection. Statistical analyses were performed using paired *t* tests. $t_{treatment} \geq 2.449$, $P \leq 0.031$ for ALPs and rewards. $n = 13$. Data are shown as the mean ± SD. *$P < 0.05$ for saline *vs*. CNO. [Colour figure can be viewed at wileyonlinelibrary.com]

Figure 7. Effect of chemogenetic activation of ZI to VTA projection neurons on feeding
Effects of CNO *vs*. saline treatment on (*A*) cumulative number of meals per hour. RM ANOVA $F_{treatment \times hour} = 0.863$, $P = 0.486$. $F_{treatment} = 5.256$, $P = 0.041$; (*B*) first meal interval. Paired *t* test $t_{treatment} = 3.100$, $P = 0.009$; and (*C*) size of the first, second and rest of meals. RM ANOVA $F_{treatment \times hour} = 6.329$, $P = 0.006$. *Post hoc* $P < 0.05$ for first meal size. *D*, satiety ratio (first meal interval/first meal size; a measure of post-meal satiety). Paired *t* test $t_{treatment} = 0.268$, $P = 0.268$. *E*, 0–1 h and 2–6 h cumulative food intake (FI). RM ANOVA $F_{treatment \times hour} = 7.603$, $P = 0.017$. *Post hoc* $P < 0.05$ at 0–1 h. $n = 13$. Data are shown as the mean ± SD. *$P < 0.05$ and **$P < 0.01$ for saline *vs*. CNO. [Colour figure can be viewed at wileyonlinelibrary.com]

meal initiation. Chemogenetic activation of ZI>VTA projection neurons showed the opposite effect on feeding, such that it promoted feeding. However, the increase in food intake resulted specifically from an increased first meal size after CNO injection. These results are in accordance with those of Zhang & van den Pol (2017), who showed that stimulation of ZI GABA neurons resulted in an intake of 35% of total daily food intake within just 10 minutes, whereas ablation of ZI GABA neurons reduced long-term food intake. An explanation for the discrepancy in feeding microstructure following activation *vs*. inactivation could be that the inactivation with TetTox was permanent and resulted in counter-regulatory mechanisms, whereas chemogenetic activation had a short-lasting effect of a few hours following CNO injection. Furthermore, the effect of chemogenetic activation of ZI>VTA projection neurons on feeding was tested in the light phase, whereas the effects on meal frequency with TetTox-inactivation were strongest in the more active dark phase.

In our chemogenetic activation study of ZI>VTA projection neurons, CNO treatment appeared to induce an acute hunger effect because the first but not the second meal size was increased, which resulted in a significant increase in cumulative food intake during the first hour after food return only. The satiety ratio (first meal interval/first meal size) shows that post-meal satiety was not affected by CNO treatment, indicating that, as a result

of the larger first meal size with CNO, rats might have felt sated for a longer time, and therefore initiated their second meal after a longer first meal interval. Thus, in line with the results of Zhang & van den Pol (2017), chemogenetic activation of ZI>VTA projection neurons specifically induced an acute hunger effect, resulting in a binge. TetTox-inactivation of these neurons appeared to have an opposite, long-term suppressing effect on hunger, as indicated by the lower meal initiation, which was inadequately compensated for by an increase in meal size.

Regulation of food intake with regard to body weight by ZI>VTA projection neurons. TetTox-inactivation of ZI-region neurons projecting to the VTA not only resulted in a lower absolute chow intake, but also a lower chow intake per 100 g of body weight, indicating a higher metabolic efficiency. This was also apparent during food restriction, during which all rats received 4 g of chow per 100 g of body weight. Food restriction had a greater impact on body weight gain in control rats compared to TetTox rats, which led to convergence of the body weights of the two groups. Previously, lesioning of the ZI was also shown to reduce the ratio of food intake to body weight (McDermott & Grossman, 1979). Similar to ZI lesioned rats (McDermott & Grossman, 1979), rats with TetTox-inactivation of ZI to VTA projection neurons maintained a body weight that was consistently lower than that of control rats after surgery, despite the higher metabolic efficiency, which may reflect the establishment of a lower postsurgical body weight set-point.

The higher metabolic efficiency following TetTox-inactivation of the ZI-region to VTA projection neurons probably provides a compensatory mechanism for the lower action initiation towards food that was reflected in the lower motivation to work for food and lower meal initiation. The ability to adjust food intake to the caloric density of diets was previously not affected by ZI lesioning (McDermott & Grossman, 1979). In accordance, TetTox rats still increased their food reward seeking in times of reduced food availability during FR. Thus, the ZI is not necessary for the coupling between metabolic needs and feeding initiation, although it generally facilitates action initiation towards feeding via its projections to the VTA.

The reduced core body temperature in rats with TetTox-inactivation of the ZI-region to VTA projection neurons could explain their higher metabolic efficiency. A lower core body temperature might be a consequence of the lower food intake, acting as a compensatory mechanism to conserve energy. Because of the permanent inactivation of the ZI-region to VTA projection neurons, it was impossible to disentangle cause and consequence of TetTox-inactivation on food intake *vs*. core body temperature. The strong relationship between food intake
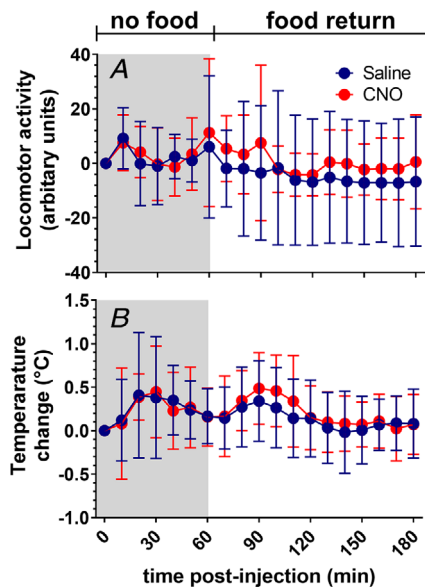
Figure 8. Effect of chemogenetic activation of ZI to VTA projection neurons on locomotor activity and core body temperature

The effect of CNO *vs*. saline treatment on (*A*) the delta change in locomotor activity and (*B*) core body temperature, in the presence and absence of food. RM ANOVA $F_{treatment} \geq 0.072$, $P \geq 0.265$. $n = 13$. Data are shown as the mean $\pm$ SD. [Colour figure can be viewed at wileyonlinelibrary.com]

and core body temperature, which was most apparent during the active feeding period (dark phase), suggests that a reduced core body temperature might be a consequence of the lower food intake. TetTox rats were still able to adapt their core body temperature in response to a metabolic challenge (as assessed by FR), suggesting normal temperature regulation upon food restriction. To investigate the role of ZI>VTA projection neurons in thermoregulation more precisely, we chemogenetically activated these neurons in the absence of food, aiming to prevent interference with feeding. Chemogenetic activation of these neurons did not affect core body temperature, suggesting that the reduction in core body temperature following TetTox-inactivation of the ZI-region to VTA projection neurons represents a compensatory response to reduced food intake rather than a direct effect of TetTox-inactivation on core body temperature.

Character of ZI input on dopaminergic neurons in the VTA. Although the VTA also contains GABAergic (∼30%) and glutamatergic (∼2–10%) neurons, the majority of neurons are dopaminergic (60–70%) and these neurons are implicated in feeding (van Zessen *et al.* 2012, Meye and Adan, 2014, Ferrario *et al.* 2016). Activation of DA neurons in the VTA has been shown to drive activational (rather than directional) aspects of motivation for food because it increases responding on both the active and inactive levers under a PR schedule of reinforcement (Boekhoudt *et al.* 2018), as well as general activity (Wang *et al.* 2013, Boender *et al.* 2014, Boekhoudt *et al.* 2016). Because chemogenetic activation of ZI>VTA projection neurons increased responding on the active but not inactive lever in PR testing and did not affect general locomotor activity, input from the ZI to VTA DA neurons appears to confine the facilitation of general action initiation towards a food-directed action initiation. This idea is supported by the TetTox-inactivation findings.

With regard to feeding microstructure, VTA DA neurons were previously shown to facilitate both the initiation and cessation of feeding behaviour by simultaneously increasing meal frequency and reducing meal size (Boekhoudt *et al.* 2017). Our data suggest that input from the ZI onto VTA DA neurons facilitates both the initiation and continuation of feeding because a loss of ZI input via TetTox-inactivation of the ZI-region to VTA projection neurons resulted in lower meal initiation, and the short-lasting chemogenetic activation of ZI>VTA projection neurons increased first meal size.

The neurochemical character of the cells in the ZI that provide input onto the VTA to promote action initiation towards feeding remains to be determined. The ZI is a brain area with an exceptionally diverse range of neurochemically defined cell types, yet GABAergic and glutamatergic cells are both quite abundant (Mitrofanis, 2005). Because the (in)activation of ZI(-region) neurons projecting to the VTA had similar effects on feeding behaviour as described for (in)activation of ZI GABA neurons (Zhang & van den Pol, 2017) [i.e. activation substantially promoted short-term (<10 min) feeding and inactivation reduced long-term feeding], the ZI might provide GABAergic input onto VTA neurons to regulate feeding behaviour. The ZI was shown to provide major input on VTA DA neurons (Ogawa *et al.* 2014). Inhibitory GABAergic input onto VTA DA neurons may confine DA signalling in the VTA to the regulation of food-related action initiation (instead of general action initiation). In addition, the ZI might also provide GABAergic input onto VTA GABA neurons because the ZI is not restricted to only innervating DA neurons in the VTA (Gonzalez *et al.* 2012 *vs.* Ogawa *et al.* 2014) and VTA GABA neurons interact locally to regulate DA neurons (McCutcheon, 2015).

Technical challenges in modulating ZI>VTA projection neurons. The results of the TetTox-inactivation study should be interpreted with two limitations in mind: (i) that we did not specifically target the ZI, but the ZI-region, and (ii) that TetTox-GFP expression was assessed at the mRNA level instead of the protein level. Perhaps we did not observe TetTox-GFP at the protein level because rats were killed a long time (29 weeks) after virus injections. The presence of TetTox-GFP mRNA expressing neurons in the ZI-region indicates that TetTox expression in neurons does not lead to cell death, as was previously reported (Carter *et al.* 2015). We speculate that permanent blockade of synaptic transmission by TetTox eventually results in blockade of translation; for example, as a result of ER stress resulting from the overexpression of TetTox transcripts and/or accumulation of non-released proteins. Of note, in our pilot study, we did observe TetTox-GFP protein in the ZI in rats that were killed 17 weeks after virus injections, comprising a time-period similar to that for the behavioural data presented in the present study. To independently confirm the results of the TetTox study, we chemogenetically activated ZI>VTA projection neurons, and thereby specifically targeted the ZI instead of the ZI-region. We chose to activate rather than inhibit ZI>VTA projection neurons because it is technically more difficult to inhibit a neuronal projection than to activate one (Carter *et al.* 2015) and we aimed to determine whether the modulation of feeding by ZI>VTA projection neurons is bidirectional.

Conclusions

In the present study, we show for the first time that the ZI regulates feeding behaviour via its projections to the VTA. Activity of the projection from ZI>VTA promotes feeding by facilitating specific action initiation towards food, as

reflected in both food-motivated behaviour and meal frequency. This may largely result from ZI modulation of VTA DA neurons. ZI>VTA projection neurons do not control general activity or directly modulate core body temperature, pointing to a specific role for ZI>VTA projection neurons in the facilitation of food-related action initiation. These findings provide new insights into the neurobiology of feeding behaviour, which may have implications for the development of novel treatments for eating disorders and obesity.

References

Amami P, Dekker I, Piacentini S, Ferre F, Romito LM, Franzini A, Foncke EM & Albanese A (2015). Impulse control behaviours in patients with Parkinson's disease after subthalamic deep brain stimulation: de novo cases and 3-year follow-up. *J Neurol Neurosurg Psychiatry* **86**, 562–564.

Berridge KC (2007). The debate over dopamine's role in reward: the case for incentive salience. *Psychopharmacology* **191**, 391–431.

Boekhoudt L, Omrani A, Luijendijk MC, Wolterink-Donselaar IG, Wijbrans EC, van der Plasse G & Adan RA (2016). Chemogenetic activation of dopamine neurons in the ventral tegmental area, but not substantia nigra, induces hyperactivity in rats. *Eur Neuropsychopharmaco* **26**, 1784-1793.

Boekhoudt L, Roelofs TJM, de Jong JW, de Leeuw AE, Luijendijk MCM, Wolterink-Donselaar IG, van der Plasse G & Adan RAH (2017). Does activation of midbrain dopamine neurons promote or reduce feeding? *Int J Obes (Lond)* **41**, 1131–1140.

Boekhoudt L, Wijbrans EC, Man JHK, Luijendijk MCM, de Jong JW, van der Plasse G, Vanderschuren LJMJ & Adan RAH (2018). Enhancing excitability of dopamine neurons promotes motivational behaviour through increased action initiation. *Eur Neuropsychopharmacol* **28**, 171–184

Boender AJ, de Jong JW, Boekhoudt L, Luijendijk MC, van der Plasse G & Adan RA (2014). Combined use of the canine adenovirus-2 and DREADD-technology to activate specific neural pathways in vivo. *PLoS One* **9**, e95392.

Campos CA, Bowen AJ, Han S, Wisse BE, Palmiter RD & Schwartz MW (2017). Cancer-induced anorexia and malaise are mediated by CGRP neurons in the parabrachial nucleus. *Nat Neurosci* **20**, 934–942.

Carter ME, Han S & Palmiter RD (2015). Parabrachial calcitonin gene-related peptide neurons mediate conditioned taste aversion. *J Neurosci* **35**, 4582–4586.

Cone JJ, Chartoff EH, Potter DN, Ebner SR & Roitman MF (2013). Prolonged high fat diet reduces dopamine reuptake without altering DAT gene expression. *PLoS One* **8**, e58251.

Ferrario CR, Labouebe G, Liu S, Nieh EH, Routh VH, Xu S & O'Connor EC (2016). Homeostasis meets motivation in the battle to control food intake. *J Neurosci* **36**, 11469–11481.

Gonzalez JA, Jensen LT, Fugger L & Burdakov D (2012). Convergent inputs from electrically and topographically distinct orexin cells to locus coeruleus and ventral tegmental area. *Eur J Neurosci* **35**, 1426–1432.

Hnasko TS, Perez FA, Scouras AD, Stoll EA, Gale SD, Luquet S, Phillips PE, Kremer EJ & Palmiter RD (2006). Cre recombinase-mediated restoration of nigrostriatal dopamine in dopamine-deficient mice reverses hypophagia and bradykinesia. *Proc Natl Acad Sci U S A* **A103**.

Huang YH & Mogenson GJ (1974). Differential effects of incertal and hypothalamic lesions on food and water intake. *Exp Neurol* **43**, 276–280.

Johnson PM & Kenny PJ (2010). Dopamine D2 receptors in addiction-like reward dysfunction and compulsive eating in obese rats. *Nat Neurosci* **13**, 635–641.

Kelley AE, Baldo BA, Pratt WE & Will MJ (2005). Corticostriatal-hypothalamic circuitry and food motivation: integration of energy, action and reward. *Physiol Behav* **86**, 773–795.

Kendrick KM, Baldwin BA, Cooper TR & Sharman DF (1986). Uric acid is released in the zona incerta of the sub-thalamic region of the sheep during rumination and in response to feeding and drinking stimuli. *Neurosci Lett* **70**, 272–277.

Kendrick KM, Hinton MR & Baldwin BA (1991). GABA release in the zona incerta of the sheep in response to the sight and ingestion of food and salt. *Brain Res* **550**, 165–168.

la Fleur SE, Luijendijk MC, van der Zwaal EM, Brans MA & Adan RA (2014). The snacking rat as model of human obesity: effects of a free-choice high-fat high-sugar diet on meal patterns. *Int J Obes* **38**, 643–649.

la Fleur SE, Vanderschuren LJ, Luijendijk MC, Kloeze BM, Tiesjema B & Adan RA (2007). A reciprocal interaction between food-motivated behavior and diet-induced obesity. *Int J Obes* **31**, 1286–1294.

McCutcheon JE (2015). The role of dopamine in the pursuit of nutritional value. *Physiol Behav* **152**, 408–415.

McDermott LJ & Grossman SP (1979). Regulation of calorie intake in rats with rostral zona incerta lesions: effects of caloric density or palatability of the diet. *Physiol Behav* **23**, 1135–1140.

Meye FJ & Adan RA (2014). Feelings about food: the ventral tegmental area in food reward and emotional eating. *Trends Pharmacol Sci* **35**, 31–40.

Mitrofanis J (2005). Some certainty for the "zone of uncertainty"? Exploring the function of the zona incerta. *Neuroscience* **130**, 1–15.

Naef L, Pitman KA & Borgland SL (2015). Mesolimbic dopamine and its neuromodulators in obesity and binge eating. *CNS Spectr* **20**, 574–583.

Nguyen DM & El-Serag HB (2010). The epidemiology of obesity. *Gastroenterol Clin North Am* **39**, 1–7.

Ogawa SK, Cohen JY, Hwang D, Uchida N & Watabe-Uchida M (2014). Organization of monosynaptic inputs to the serotonin and dopamine neuromodulatory systems. *Cell Rep* **8**, 1105–1118.

Romieu I, Dossus L, Barquera S, Blottiere HM, Franks PW, Gunter M, Hwalla N, Hursting SD, Leitzmann M, Margetts B, Nishida C, Potischman N, Seidell J, Stepien M, Wang Y, Westerterp K, Winichagoon P, Wiseman M & Willett WC & IARC working group on Energy Balance and Obesity (2017). Energy balance and obesity: what are the main drivers? *Cancer Causes Control* **28**, 247–258.

Salamone JD & Correa M (2012). The mysterious motivational functions of mesolimbic dopamine. *Neuron* **76**, 470–485.

Solinas M & Goldberg SR (2005). Motivational effects of cannabinoids and opioids on food reinforcement depend on simultaneous activation of cannabinoid and opioid systems. *Neuropsychopharmacology* **30**, 2035–2045.

Stice E, Yokum S, Blum K & Bohon C (2010). Weight gain is associated with reduced striatal response to palatable food. *J Neurosci* **30**, 13105–13109,.

van der Plasse G, van Zessen R, Luijendijk MC, Erkan H, Stuber GD, Ramakers GM & Adan RA (2015). Modulation of cue-induced firing of ventral tegmental area dopamine neurons by leptin and ghrelin. *Int J Obes* **39**, 1742–1749.

van der Zwaal EM, Luijendijk MC, Evers SS, la Fleur SE & Adan RA (2010). Olanzapine affects locomotor activity and meal size in male rats. *Pharmacol Biochem Behav* **97**, 130–137.

van Zessen R, van der Plasse G & Adan RA (2012). Contribution of the mesolimbic dopamine system in mediating the effects of leptin and ghrelin on feeding. *Proc Nutr Soc* **71**, 435–445.

Volkow ND, Wang GJ, Fowler JS & Telang F (2008). Overlapping neuronal circuits in addiction and obesity: evidence of systems pathology. *Philos Trans R Soc Lond B Biol Sci* **363**, 3191–3200.

Wang GJ, Volkow ND, Logan J, Pappas NR, Wong CT, Zhu W, Netusil N & Fowler JS (2001). Brain dopamine and obesity. *Lancet* **357**, 354–357.

Wang S, Tan Y, Zhang JE & Luo M (2013). Pharmacogenetic activation of midbrain dopaminergic neurons induces hyperactivity. *Neurosci Bull* **29**, 517–524.

Wise RA (2004). Dopamine, learning and motivation. *Nat Rev Neurosci* **5**, 483–494.

Zahodne LB, Susatia F, Bowers D, Ong TL, Jacobson CE, 4th, Okun MS, Rodriguez RL, Malaty IA, Foote KD & Fernandez HH (2011). Binge eating in Parkinson's disease: prevalence, correlates and the contribution of deep brain stimulation. *J Neuropsychiatry Clin Neurosci* **23**, 56–62.

Zhang X & van den Pol AN (2017). Rapid binge-like eating and body weight gain driven by zona incerta GABA neuron activation. *Science* **356**, 853–859.

Zhou QY & Palmiter RD (1995). Dopamine-deficient mice are severely hypoactive, adipsic, and aphagic. *Cell* **83**, 1197–1209.

Additional information

Data availability statement

The datasets supporting the conclusions of this article are stored at UMCU facilities (according to UMCU's data management plan) and are available from the corresponding author upon reasonable request.

Competing interests

The authors declare that they have no competing interests.

Author contributions

The experiments were performed at the Brain Center Rudolf Magnus, Department of Translational Neuroscience, University Medical Center Utrecht, Utrecht University, The Netherlands. KG, GP and RA conceived and designed the experiments. KG, EH, MN, ML and GP were responsible for the collection, analysis and interpretation of data from the TetTox-inactivation experiments. KG, MN, ML and GPwere responsible for the collection, analysis and interpretation of data from the chemogenetic activation experiments. KG wrote the manuscript. GP and RA critically revised the manuscript. All authors have approved the final version of the manuscript and agree to be accountable for all aspects of the work. All persons designated as authors qualify for authorship, and all those who qualify for authorship are listed.

Funding

Acknowledgements

Keywords

DREADD, feeding, motivation, tetanus toxin light chain, ventral tegmental area, zona incerta

Supporting information

Additional supporting information may be found online in the Supporting Information section at the end of the article.

Statistical Summary Document